Structure of colloidal particles in water-oil mixtures stabilized by polymeric emulsifiers. 3. Hydrodynamic properties

S. Candau
Laboratoire d'Acoustique Moléculaire Equipe de Recherche Associée au C.N.R.S., Université Louis Pasteur, 4, rue Blaise Pascal, Strasbourg, France.

J. Boutillier and F. Candau
Centre de Recherches sur les Macromolécules, 6, rue Boussingault, Strasbourg, France.
(Received 16 February 1979)

The micellar properties of water-oil mixtures stabilized by polystyrene-poly(ethyleneoxide) graft copolymers, in the presence of an alcohol, have been investigated by quasielastic scattering of laser light and viscometry. The mean size, aggregation number, polydispersity and swelling degree of the polymeric micelles have been deduced for a series of copolymers as a function of the solvent composition. Both size and aggregation number are strongly dependent on the toluene/water ratio. The swelling degree of particles is primarily controlled by the weight ratio polystyrene/poly(ethylene-oxide).

The hydrodynamic transport properties of particles suspended in fluids have been considered both theoretically[1-10] and experimentally[11-14] by many workers. Most of the investigations, however, have been concerned with highly dilute suspensions or solutions for which concentration effects due to particle interactions are negligible. The effect of interaction is removed by extrapolating measurements of, for instance, diffusion coefficients or sedimentation coefficients to zero solution concentration, thus giving single particle value. The information which is generally obtained from these experiments is the hydrodynamic volume of the particle which, in the simplest case of hard sphere solute can be identified to its geometrical volume.

The calculation of finite concentration transport properties is much more intricate because one must deal with the many body problem of N particles interacting via both intermolecular and hydrodynamic forces. The difficulties associated with this problem are so severe that the case which has been most investigated is that of simple hard sphere suspensions.

The polymeric systems considered in this series of papers can be identified with a reasonable approximation to hard spheres suspensions, since the dispersed particles exhibit generally a rather compact structure, as evidenced by the electron microscopy and neutron scattering experiments reported before. Therefore hydrodynamic techniques can provide some useful information on the micellar structure of the suspended particles.

In our study, we employed the technique of quasi elastic light scattering spectroscopy (*QELS*) which allows one to measure the translational diffusion coefficients of the particles and yet has only recently been applied to the study of micellar solutions.[15-20] In addition, *QELS* offers a quantitative characterization of colloidal polydispersity.[21-22] In the high dilution limit, the Stokes-Einstein relation[1] can be used to relate the diffusion coefficient to the hydrodynamic radius of the particles.

Moreover, by employing viscosity measurements and assuming a hard sphere model we have determined the degree of swelling of the dispersed particles. These results in conjunction with the hydrodynamic radii allowed us to deduce the corresponding aggregation numbers of copolymer micelles as a function of the compositions of both amphiphilic copolymer and ternary solvent mixture.

The self-consistency of our approach can be checked by comparing the two sets of data obtained independently from neutron scattering and hydrodynamic experiments.

Furthermore, the data reported in part 1, relating to the composition of the external continuous phase, in conjunction with the degrees of swelling of the particles, yield the composition of the solvent mixture inside the micellar particles, thus completing our knowledge of the water-oil transparent systems stabilized by amphiphilic copolymers.

THEORETICAL

Since the interpretation of the experimental data is dependent upon an underlying theoretical model, it is appropriate to give a very brief account of the basic theory, indicating the assumptions being made. In the following, we will consider separately the theoretical treatments of the polarized light scattering spectrum and the viscosity for suspensions of hard spheres since the interactions between particles occur in a different way in the two sets of experiments.

Intensity correlation function of laser light scattered from hard spheres suspensions

Measurements of the autocorrelation function of light quasielastically scattered from solutions or suspensions of particles enables determination of the following dynamical structure factor:

$$S(\underline{K}, t) = \langle \delta c(\underline{K}, t) \delta c^*(\underline{K}, 0) \rangle \quad (1)$$

0032-3861/79/101237-08$02.00

where $\delta c(\underset{\sim}{K}, t)$ is the spatial Fourier transform of the local particle concentration fluctuations at time t and for a momentum transfer $\underset{\sim}{K}$ of scattered light. The magnitude of $\underset{\sim}{K}$ is given by:

$$K = \frac{4\pi \sin\theta/2}{\lambda/n} \quad (2)$$

where θ is the scattering angle, λ is the wavelength of the incident light in vacuum, and n is the refractive index of the scattering medium.

At the high dilution limit, the concentration fluctuation can be described by a single particle diffusion equation and the normalized dynamic factor structure $g^{(1)}(t)$ has the well known form:[23]

$$g^1(t) = \left(\frac{S(K,t)}{S(K,0)}\right) = e^{-D_0K^2t} \quad (3)$$

where D_0 is the translational diffusion coefficient of the particle in the limit $c = 0$. When the particles are much larger than the solvent molecules, D_0 is given by the Stokes-Einstein relationship:[1]

$$D_0 = \frac{k_BT}{6\pi\eta_0R_p} \quad (4)$$

where k_B is the Boltzman constant, T the temperature, η_0 the viscosity of the solvent and R_p the radius of the particle.

When dealing with hard spheres suspensions of finite concentrations, the dynamical structure factors must be derived from a full N-body diffusion equation. Potentially, the most important dynamical concentration effect in the suspension might arise from the long range hydrodynamic interactions. Recently, Altemberger and Deutch[24] have analysed this problem and shown that for incompressible liquids, the long range interaction terms in the N-particle diffusion equation do not contribute to $S(K, t)$ which is still given by equation 3. On the other hand, these authors have shown that, when short range forces are taken into account and the incompressibility assumption is relaxed, $S(K, t)$ can be approximated, for sufficiently small radii ($KR_P \ll 1$) as:

$$S(K, t) = S(K, 0)\exp(-DK^2t) \quad (5)$$

with an effective concentration dependent diffusion constant given by:

$$D = D_0(1 + 2\Phi_2) \quad (6)$$

where Φ_2 is the volume fraction of the dispersed particles.

The problem of the concentration dependence of the diffusion constant has also been treated from a macroscopic thermodynamic approach.[9,25] The effect of concentration on both chemical potential μ and friction coefficient f of the suspension is represented by a virial expansion leading to:

$$D = \frac{\partial\mu/\partial c}{f} = D_0\left|1 + (8 - K_f)\Phi_2 + \ldots\right| \quad (7)$$

The coefficient 8 appearing in the brackets arises from excluded volume interactions due to the finite size of the particles.

The friction virial K_f has been calculated from a microscopic approach. The predicted value of K_f ranges from 6.55[10] through 6.77,[7] and 6.86[8] to 7.2.[9] equation (6) yields: $K_f = 6$.

It can be seen from equation 7 that for hard spherical particles, the individual effects on the concentration dependence of D, of $(\partial\mu/\partial c)$ and f almost cancel.

Thus D in such systems can be expected to show a positive but much smaller concentration dependence than for instance, the viscosity or the sedimentation coefficient (which is proportional to $1/f$).

This result has been confirmed experimentally in several systems.[23,26] However the virial coefficient $(8 - K_f)$ of the diffusion constant expansion was generally found smaller than the predicted value which ranges from 0.8 to 2. The discrepancy between theory and experiment may be attribited to neglect of attractive forces between spheres which tend to compensate the excluded volume effect.[7,25]

Viscosity of hard spheres suspensions

Up to moderate concentration, the viscosity of the suspension is adequately represented by the displayed terms of

$$\eta/\eta_0 = 1 + 2.5\,\Phi_2 + K'\Phi_2^2 + \ldots \quad (8)$$

In the high dilution limit equation (8) reduces to the familiar Einstein's formula[1]

$$\eta = \eta_0(1 + 2.5\,\Phi_2) \quad (9)$$

Numerous theories have been developed in efforts to estimate the numerical value of the coefficient K' in the quadratic term in Φ_2 of equation (8). Unfortunately there is no agreement on the principles by which K' is to be calculated. The numerical estimates of K' range from 4.3[6,7] through 4.8[27] to 12.6.[5] The fit of equation (8) to the experimental data gives values of K' varying between 7.35 and 14. They are generally higher than the predicted values but that (12.6) of the Simha's theory. This discrepancy can be attributed to neglect of attractive forces between spheres, since only the excluded volume effect and hydrodynamic interactions have been taken into account in the theoretical derivations. The effect of attractive forces in the concentration dependence of the viscosity may depend considerably on the nature of the investigated system. Therefore, in practice, it seems more reliable to determine Φ_2 from a fitting procedure of equation (9) to the experimental data with variables Φ_2 and K'. This method of course requires a dilution procedure.

By combining viscosity and quasielastic light scattering one can obtain both the radius and the swelling degree of the suspended particles.

EXPERIMENTAL

Materials

The characteristics of the investigated systems were described in detail in the preceding papers. The solutions were centrifuged for 2 h at 15 000 rev/min to exclude dust before use. All the measurements were performed at 22°C.

Quasielastic light scattering measurements

A Spectra-Physics argon-ion laser (λ = 4880 Å) was used in conjunction with a 48 channel clipped digital auto-

correlator (Precision Devices and Systems LTD Malvern type K 7023) for measuring the autocorrelation function of the scattered light intensity. The scattering angle was varied from 20° to 120° by relocation of the photomultiplier tube which was mounted on a rotatable platform. The experimental data were transferred to an online computer and processed using the methods of cumulants[21-23] to provide a statistical measure of decay rates Γ_i. This distribution was characterized through its two first moments which are related to the average decay rate $\bar{\Gamma}$ and the variance V whose meaning will be discussed below. The coefficient $\bar{\Gamma}$ is given by:

$$\bar{\Gamma} = \Sigma G_i \Gamma_i \tag{10}$$

where G_i represents the fraction of the total intensity scattered by component i and is given by

$$G_i = \frac{c_i M_i P_i}{\Sigma c_i M_i P_i} \tag{11}$$

where M_i, P_i and c_i refer to the molecular weight, the form factor for light scattering and the concentration of component i.

The variance V is a measure of the width of the distribution and is related to the second moment of the distribution $\overline{\Gamma^2} = G_i I_i^2$ by the relationship:

$$V = (\overline{\Gamma^2} - \bar{\Gamma}^2)/\bar{\Gamma}^2 \tag{12}$$

From the average decay rate $\bar{\Gamma}$ and the appropriate value of K, the mean diffusion coefficient D_p of the micellar particles was obtained. The refractive index n needed for the calculation of K (equation 2) was measured by using an Abbé refractometer. In our study we had also to consider the case where the decay of fluctuations occurs via two uncorrelated relaxation processes, one having decay rate Γ_1 and the other Γ_2. The corresponding correlation function of the photocurrent $C_i(\tau)$ obtained in the self beat mode has the following form:[29]

$$C_i(\tau) = e\langle i\rangle \delta(\tau) + \langle i\rangle^2 \left[1 + \frac{A_1 e^{-2\Gamma_1\tau} + 2A_1A_2 e^{-(\Gamma_1+\Gamma_2)\tau} + A_2^2 e^{-2\Gamma_2\tau}}{(A_1 + A_2)^2}\right] \tag{13}$$

where $\langle i\rangle$ is the average photocurrent, e the charge of the electron, A_1 and A_2 the fractions of the total light intensity scattered, associated with the relaxation processes (1) and (2) respectively.

The last term of equation 13 can be approximated to a single exponential for large value of the ratio $A_1/A_2 (> 10)$. Furthermore, if the ratio Γ_1/Γ_2 exceeds a value of about 15, it is possible to analyse separately the two relaxation processes by using different sampling times of the autocorrelator.

In some experiments we have measured the power spectrum density of the scattered light by using a wave analyser (General Radio type 1910 A). A device which has been described elsewhere[28] activates the analyser only within a narrow range of photomultiplier current, in order to eliminate the problem of drifts. The output of the analyser is converted to digital signal and processed automatically using an online computer. This set up enables us to explore a rather broad range of frequencies (10-50000 Hz) with the same filter bandwidth, making thus possible to characterize in a single run, superimposed Lorentzian components of very different halfwidths. For instance, if we consider again the case of two uncorrelated relaxation processes, the theoretical self-beat spectrum $P_i(\omega)$ is given by the Fourier transform of the photocurrent autocorrelation function $G_i(\tau)$ (equation 13).

$$P_i(\omega) = \frac{e\langle i\rangle}{\pi} + \langle i\rangle^2 \delta(\omega) + \frac{2\langle i\rangle^2}{(A_1 + A_2)^2}\left[A_1^2 \frac{2\Gamma_1}{\omega^2 + (2\Gamma_1)^2} + 2A_1A_2 \frac{\Gamma_1 + \Gamma_2}{\omega^2 + (\Gamma_1 + \Gamma_2)^2} + A_2^2 \frac{2\Gamma_2}{\omega^2 + (2\Gamma_2)^2}\right] \tag{14}$$

Viscometry

The viscosity measurements were performed by using either a coaxial cylinders viscometer (Haake Rotovisco RV 3) or a capillary viscometer. In the range of shearing rates investigated, i.e. 20-300 s^{-1} the systems exhibited a Newtonian behaviour. The values of the mass per volume needed for the determination of viscosity coefficients were measured with an accuracy of 5×10^{-3} g cm^{-3} by using a densitometric beam scales based on the Archimedean principle.

EXPERIMENTAL RESULTS

Quasi elastic light scattering

In the system investigated here, the colloidal particles are suspended in a mixture of solvents. Therefore the solvent fluctuations are superimposed on the Brownian motion of the polymeric particles and the correlation function thus has the form given by equation (13) with $\Gamma_1 = D_p K^2$ and $\Gamma_2 = D_s K^2$, D_p and D_s standing for the mutual diffusion constants of the particles and the solvent mixture respectively. We have measured by *QELS* the coefficient D_s over a wide region of the homogeneous phase of the ternary solvent mixture. From the D_s value, a measure of the correlation length ξ_s of the solvent fluctuations was deduced by using the Stokes-Einstein relation

$$\xi_s = \frac{k_B T}{6\pi\eta_0 D_s} \tag{15}$$

where η_0 stands for the viscosity of the ternary mixture.

Figure 1 shows a three dimensional plot of ξ_s as a function of the composition of the solvent mixture. One can remark that ξ_s increases regularly in passing from the toluene-rich part of the binodal curve to the water-rich side. One does not observe any singularity in the vicinity of the plait point (indicated by P on the mutual solubility line). These results are in good accordance with the observation of Washburn and Beguin which showed that the size of the dispersed droplets appearing at the end points of the titration process increases also monotonically along the binodal curve from the toluene-side to the water-side.[30]

If now, for a given water-toluene ratio, the amount of 2-propanol is increases, ξ_s decreases, as shown in *Figure 1*.

The major aim of the *QELS* experiments was to determine the size of the dispersed particles in different regions of the phase diagram. This determination requires an extrapolation to zero concentration of the measured diffusion constant. For this purpose, the systems were diluted as mentioned before with a mixture of the same composition as the continuous phase. The measurements of the auto-

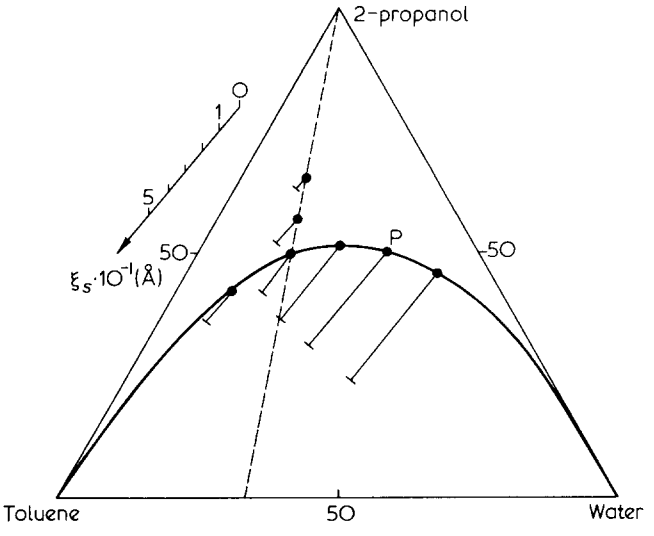

Figure 1 Three dimensional plot of ξ_S as a function of the composition of the ternary mixture. The full line represents the mutual solubility curve; *P* is the plait point (from ref. 30). The dashed straight line represents mixtures whose toluene/water ratio is constant and equal to 2/1

correlation function (or, alternatively, power spectrum of photocurrent) were performed on the systems previously investigated by electron microscopy and neutron scattering techniques.

Systems located at the vicinity of the transition line (A and B in Figure 4 of Part 1)

In the water-rich region (system B) the autocorrelation function fits a single exponential rather well. The variance ranges from $V \sim 0.01$-0.025 for sample A_4 through $V \sim 0.2$ for sample A_7 to $V \sim 0.2$ for sample A_3. The mean decay rates exhibit a K^2 dependence. Plots of the mean diffusion constant $\bar{D}$ versus concentration as derived from cumulant analysis are shown in *Figure 2*. For sample A_4, an increase of $\bar{D}$ with the dilution is observed in the low concentration range ($c < \sim 2.5\ 10^{-2}$ g cm^{-3}). This behaviour may be attributed to the influence of the solvent fluctuations rather than to a real variation of the particle diffusion

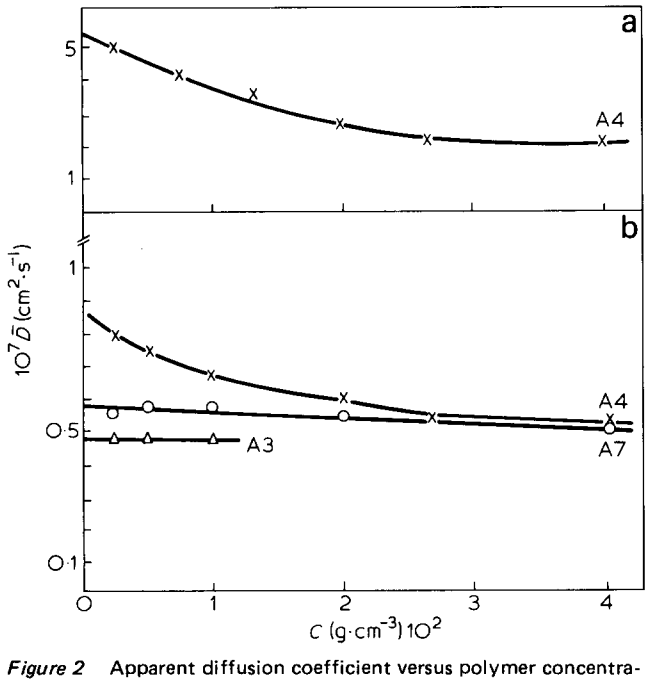

Figure 2 Apparent diffusion coefficient versus polymer concentration for systems A and B

coefficient as can be ascertained from the following considerations.

In the high concentration range, the scattering arises predominantly from the colloidal particles and accordingly the analysis of the autocorrelation function provides a measure of the diffusion constant D_p of the particle. The coefficient D_p is found to be only about four times lower than the diffusion constant D_s associated with the solvent mixture. Therefore, as the concentration decreases, the scattering from solvent fluctuations is not anymore negligible and a correct analysis of the autocorrelation function requires a fit to a sum of three exponentials according to equation (13). By using such an analysis which reduces to a three parameters fit since D_s is measured in a separate experiment, D_p is found to be independent on concentration within the experimental accuracy. For sample A_7 and A_3, the scattering from particles is predominant in the whole investigated range of concentrations and the cumulant analysis gives the correct value of D_p.

In the toluene-rich region (system A), the shape of the autocorrelation function and the mean decay rate depend strongly on the nature of the copolymer. The behaviour of system A formed from sample A_4 is similar to that observed in the water-rich side (see *Figure 2*). On the other hand, the autocorrelation function of samples A_5, A_7 and A_3 depart markedly from a single exponential behaviour and exhibits a long tail. Correlatively, the spectrum power $P_i(\omega)$ shows a non Lorentzian behaviour as illustrated in *Figure 3* relative to the sample A_3. The above results must be associated with the clusters of particles whose presence has been evidenced in the same system by electron microscopy (see Part 1, *Figure 6d*).

Systems containing an excess of 2-propanol (A' and B' in Figure 4 of Part 1)

For systems located in the region of the phase diagram far above the transition line, two components appear either in the autocorrelation function or in the power spectrum. The two corresponding decay times, whose ratio exceeds 25, were determined from a separate analysis of each component. The diffusion constant associated with the fast relaxation process was found to be equal to D_s. The diffusion constant of the particles D_p, as deduced from the decay time of the slow component is plotted in *Figure 4* as a function of the polymer concentration. The variance related to the particle polydispersity was found to be generally less than 0.025. Some samples exhibit a larger polydispersity at high concentration ($c > 2.5\ 10^{-2}$ g cm^{-3}), e.g. sample A_4 in the

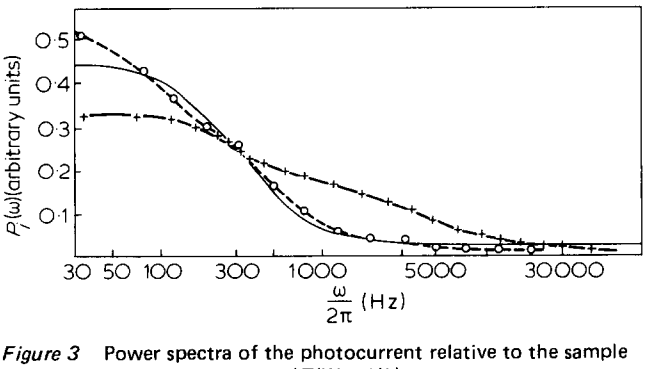

Figure 3 Power spectra of the photocurrent relative to the sample A_3 in the toluene-rich systems (T/W = 5/1).
+ Systems A, $c = 4\ 10^{-2}$ g cm^{-3} o Systems A', $c = 2.5\ 10^{-2}$ g cm^{-3}.
The full line represents the best fit of the experimental data to a single Lorentzian curve.

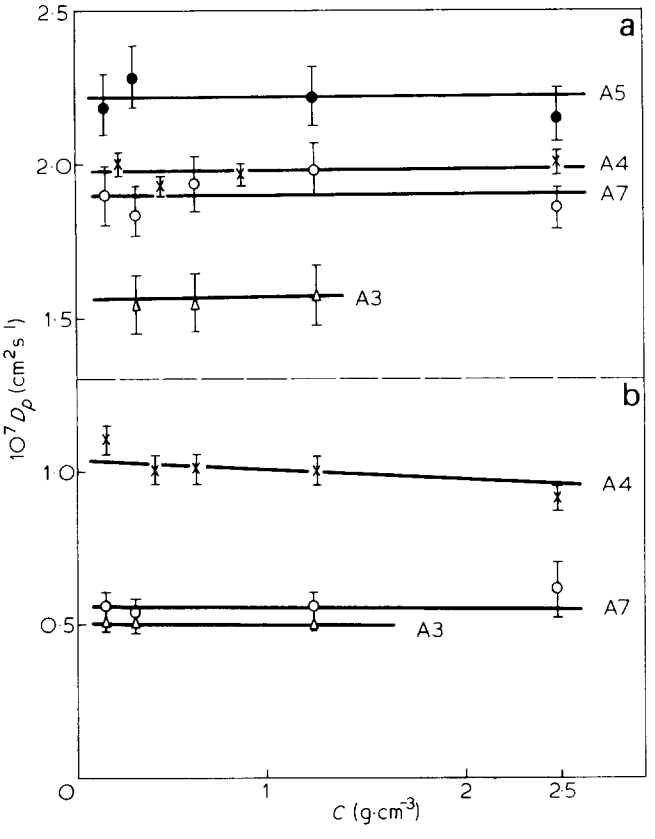

Figure 4 Diffusion coefficient versus polymer concentration for systems A′ and B′

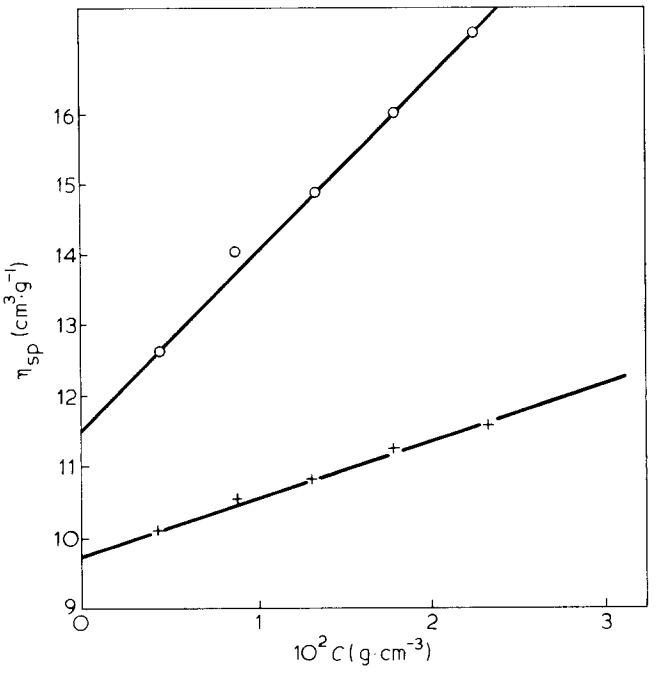

Figure 5 Specific viscosity versus polymer concentration for sample A_4
o Systems A′ + Systems B′

predominantly aqueous phase ($V \sim 0.2$) and samples A_5 and A_7 in the toluene-rich side ($V \sim 0.5$). Moreover, there is evidence of remaining clusters in the system A' obtained from sample A_3 as demonstrated by the power spectrum reported on *Figure 3*. One clearly sees in the spectrum a high frequency component which can be ascribed to the individual particle motion and a low frequency component of small amplitude characterized by a half-width of same order of magnitude as that obtained for the clustered A systems. This slow component disappears by diluting the system.

Viscometry

As outlined in the theoretical section, the relative viscosity $\eta_r = \eta/\eta_0$ of hard spheres suspensions is only function of the volume fraction Φ_2. It can be reasonably assumed in the light of the diffusion constant and neutron scattering data that the size of the dispersed particles is independent of the polymer concentration, at least in the low concentration range. Therefore, the volume fraction Φ_2 must be proportional to the polymer concentration and equation (8) can be written as follows:

$$\eta/\eta_0 = 1 + 2.5\,sc + K' s^2 c^2 \qquad (16)$$

where $s = \Phi_2/c$ represents the swelling degree (w/v) of the particles.

Following a standard procedure for studies of polymer solutions,[25] the viscosity data were analysed by plotting the specific viscosity $\eta_{sp} = \eta - \eta_0/\eta_0 c$ as a function of the polymer concentration. According to equation (16), η_s must be a linear function of c. This was found experimentally as shown in *Figure 5*, thus confirming the assumption of proportionality between the volume fraction of colloidal particles and the polymer concentration. The intercept and the slope of $\eta_{sp} = f(c)$ yield the parameters s and K' respectively. The values of s and K' relative to several systems are listed in *Table 1*.

DISCUSSION

Particle interactions

In this study, the effects of particle interactions appear through either the concentration dependence of the trans-

Table 1 Swelling degrees, interaction parameters and aggregation numbers relative to samples A_4 and A_7

Sample	Toluene-rich side							Water-rich side						
	System[a]	T/W[b]	s (cm^3·g^{-1})	K′	$\bar{N}_{vis}$[c] (1)	(2)	$\bar{N}_{SANS}$	System[a]	T/W[b]	s (cm^3·g^{-1})	K′	$\bar{N}_{vis}$[c] (1)	(2)	$\bar{N}_{SANS}$
A_4	A	5/1	5.1	12.5	3.7	2.7	2	B	1/5	4.9	4.7	45	30	18
A_7		5/1	11	10.5	–	6	3		1/5	21	3	5.5	3.5	7
A_4	A′	2/1	4.6	11.3	5.5	3.4	2	B′	1/5	3.9	5.7	22	5.7	6
A_7		2/1	9.2	12.5	1.6	1.2	1		1/11	11.6	4.7	23	40	13

[a] Systems A and B are located at the vicinity of the transition line, systems A′ and B′ contain an excess of 2-propanol.
[b] Ratio toluene/water in the ternary solvent mixture.
[c] Calculated from equation (17) with (1) $R_p = R_h$, (2) $R_p = R_G$.

port coefficients or the formation of clusters. It has been shown from the analysis of the *QELS* data that the diffusion constant of the particles does not depend on the polymer concentration. This behaviour has already been observed in other micellar systems and is generally interpreted as a consequence of the compensation between attractive and repulsive interactions.[23-26] A slight increase of D_p can be expected according to equation (7), if only hydrodynamic interactions and excluded volume effect are taken into account.

The concentration dependence of specific viscosity is much more sensitive to the particle interactions and information on the nature of these interactions can be provided from the numerical values of the constant K' of the quadratic term of the expansion of η_r (cf. equation 8).

Inspection of *Table 1* shows that K' is rather unsensitive to the nature of the copolymer but varies considerably with the composition of the system. As a general rule, the experimental values of K' for predominantly aqueous phases are rather close to 4.5 which is the average value predicted by most theories where attractive forces are neglected.[6-8]

On the other hand, the attractive interactions play a more important role in the toluene-rich systems as evidenced by the larger values of K'. The above results can be understood by considering that the attractive interactions occur mainly between the PS cores of the micelles which are surrounded by an unfavourable environment. The importance of this effect will depend on the shielding efficiency of the PEO shell which prevents further aggregation of PS. It is reasonable to assume that this shielding is more efficient when the medium outside the micelles is predominantly aqueous.

Another evidence of the attractive interactions is found in the clustering effect which appears mainly in the toluenic side of the phase diagram. Referring back to *Figure 3*, one can roughly estimate from the half-width of the power spectrum the size of the scattering objects. This size was found to be approximately 0.15 μm, that is fairly close to the typical spatial scale characterizing the clusters in the electron micrographs. It should be noticed that this scale exceeds largely the range of the inverse scattering wavevector investigated. This result means that the particles are tightly bounded in the clusters and the *QELS* experiments probe the whole motion of the cluster instead of single particle motion.

Inspection of *Table 2* shows that for sample A_4 in the predominantly aqueous phase, the *QELS* result does not provide confirmatory evidence of the clusters. This behaviour can be explained by assuming that the attractive forces between particles inside a cluster are much weaker than in the preceding case. Consequently the *QELS* experiment probes the individual particle motion.

Size of particles

In *Table 2*, we have compared the data relative to the size of the dispersed particles, as deduced from the *QELS*, *SANS* and *EM* experiments respectively. It should be first noticed that these techniques do not provide the same information. Moreover each technique has its own limitations which may originate some errors in the measurements.

The *EM* experiments give the number of average radius of the imprint. Let us recall that there is some ambiguity concerning the relationship between the size of the imprints and the real size of the particles because of the plastic deformation effect. It should also be emphasized that the data from *EM* experiments are relative to rather concentrated systems which exhibit a non negligible particle polydispersity as evidenced by the *QELS* experiments. The two major discrepancies between the *EM* data and the results of *QELS* and *SANS* experiments are observed for samples A_3 and A_7 (in systems A') which are characterized by a rather high micellar polydispersity.

The *QELS* experiments provide a measure of the hydrodynamic radius R_h of the particles. For hard, or hollow spheres, R_h is equal to the radius R_p of the particle. In the case of polydisperse systems, the cumulant analysis provides a z average of $D_p \sim (R_h)^{-1}$.

The *SANS* experiments lead to the determination of the radius of gyration R_G of the particle. The relationship between R_G and R_p depends on the micellar structure of the particle. For a very compact micelle behaving as a hard sphere $R_G = (3/5)^{1/2} R_p$. On the other hand, if we assume that the two segregated sequences of the copolymer form a compact shell surrounding a cavity filled with a solvent mixture, then $R_G = R_p$. Several causes of errors may have disturbed the *SANS* measurements. Firstly, some determinations of R_G were performed at the very end of the 'Guinier' scattering vector range. Secondly, the value of R_G obtained in the case of clustered systems (A, sample A_7) may be overestimated because of interference effects between particles. Finally we must consider that the isotopic substitution of solvents might modify their preferential solvation by the two sequences of the copolymer.

On account of these considerations, the agreement between the data obtained from the three techniques can be considered as satisfactory. Inspection of *Table 2* shows

Table 2 Radii (Å) of the dispersed particles measured by means of *EM, SANS* and *QELS* techniques for the different systems investigated

Method	Toluene-rich side					Water-rich side				
Copolymer	System[a]	T/W[b]	R (*EM*)	R_G (*SANS*)	R_h (*QLS*)	System[a]	T/W[b]	R (*EM*)	R_G (*SANS*)	R_h (*QLS*)
A_4	A	5/1	55	63	70	B	1/5	clusters	130	150
A_5	A	5/1	clusters	–	*	B	1/5	200	–	–
A_7	A	5/1	clusters	125	*	B	1/5	200	130	150
A_3	A	5/1	clusters	–	*	B	1/5	230	–	160
A_4	A′	2/1	60	62	73	B′	1/5	150	70	110
A_5	A′	2/1	95	–	65	B′	1/5	–	–	–
A_7	A′	2/1	220	69	76	B′	1/11	250	240	200
A_3	A′	2/1	180	–	95	B′	1/5	210	–	200

[a] Systems A and B are at the vicinity of the transition line systems A′ and B′ contain a high 2-propanol content.
[b] Ratio toluene/water in the ternary solvent mixture.
*Strongly non exponential autocorrelation function.

that the size of the particles is mainly controlled by the ratio T/W of the solvent mixture, the values obtained in the water-side systems being much larger than in the toluene-side. On the average the size does not show a strong dependence on the nature of the copolymer.

Swelling degree of the particles and aggregation number

The data reported in *Table 1* show that the swelling degree of the particles depends substantially on the amphiphilic nature of the copolymer. For a given solvent composition, the compound A_7 which is more hydrophilic than sample A_4 exhibits a larger swelling. Furthermore s increases with increasing the amount of water for sample A_7 whereas it decreases slightly for sample A_4. The swelling degree used in conjunction with the corresponding radius of the particle provides a measure of the aggregation number $\bar{N}$ according to:

$$\bar{N} = \frac{4\pi R_p^3 . \mathcal{N}}{3M_w s} \qquad (17)$$

where $\mathcal{N}$ is the Avogadro number.

The aggregation numbers were calculated from equation (17) by using either R_h or R_G as an estimate of R_p and the values were compared with the results obtained from *SANS* experiments (see *Table 1*). Either set of experiments leads to the same general behaviour primarily characterized by the fact that the aggregation number grows as the amount of water is increased. The major uncertainty in the determination of $\bar{N}$ from equation (17) comes from the uncertainty in the size of the particles. Moreover the determination of s was based on the hard spheres model. In this regard, the *SANS* data show that there is only one case (sample A_4 in system B') where the hard sphere behaviour ($n \sim 4$) is observed in a large momentum range ($0.03 < q < 0.1$) (see *Table 2* of Part 2). This system is nevertheless characterized by a substantial degree of swelling. From this observation, the possibility cannot be excluded that the double layer of PEO and PS forms a compact shell which would trap a certain amount of the solvent mixture.

CONCLUSION

The studies presented in this series of papers provide some insight into the role played by amphiphilic copolymers in the formation of optically clear water–toluene systems in the presence of an alcohol. Such systems have been shown to be located in two distinct regions of the phase diagram.

The first domain appears in the toluene-rich side of the phase diagram. The corresponding overall compositions of the quaternary mixture are fairly close to the typical compositions of the microemulsions obtained using a soap as a surfactant. In this case, about all the available water is trapped within the micelles. This requires a rather ordered arrangement of the shell of the micelle. A detailed investigation of the properties of these systems is in progress.

The second domain, characterized by a larger content of 2-propanol in the system, corresponds to the systems previously observed by Riess *et al.*[31] who used other amphiphilic copolymers, and called by these authors 'polymeric microemulsions'. The dialysis experiments, presented in *Part 1* allowed us to show that the enhancement of the water-oil solubility was due to a preferential solvation of the two segregated components of copolymer by the ternary mixture of solvents in variable composition, contrary to the classical microemulsions where one specific solvent is almost entirely trapped. A detailed investigation of the structure of the dispersed polymeric particles has been carried out using several complementary techniques.

The *EM* experiments have shown that the dispersed phase consists of spherical micelles. At some specific compositions of the solvent mixtures, these micelles aggregate to form clusters. This phenomenon, confirmed by *QELS* experiments, may be of interest because the formation of such clustered structures has been invoked to explain the *QELS* results obtained on micellar solutions of sodium dodecylsulphate at high ionic strength.[20] The latter systems and the non-ionic polymeric systems investigated here are comparable since at high ionic strength, the Coulomb potential is screened and the Van der Waals attractions become predominant.

The *SANS* experiments have given information on the short range conformation of the copolymer molecules. Furthermore they have led to the determination of the size and the aggregation number of the copolymer in the micelles.

Finally, the *QELS* and viscometry experiments have provided an independent characterization of the micellar parameters and complementary information on the particle interactions. The data permits us to give a semi quantitative model of the polymeric micelles. These micelles consist of an inner layer of PS and an outer layer of PEO whatever the T/W ratio. The question whether the PS layer fills all the core of the micelle or it surrounds a cavity filled with a solvent mixture is still open. The swelling degree of the particles is fairly high and goes generally along with the size and the aggregation number of the particles. The two parameters which mainly control as well the molecular conformation of the copolymer in the micelle as the overall structure of the micelle are the ratio T/W and the weight ratio PS/PEO. The latter parameter can be considered as the equivalent for polymeric microemulsions of the *HLB* parameter[32] used for classical microemulsions.

REFERENCES

1 Einstein, A. *Ann. Physik* 1906, **19**, 289; 1911, **34**, 591
2 Stokes, G.G. Mathematical and Physical Papers **III**, University Press, Cambridge, (1901) p. 59
3 Mooney, M. *J Colloid Sci* 1951, **6**, 162
4 Brinkham, H.C. *J Chem Phys* 1952, **20**, 571
5 Simha, R. *J Appl Phys* 1952, **23**, 1020
6 Peterson, J.M. and Fixman, M. *J Chem Phys* 1963, **39**, 2516
7 Mou, Chung Yuan and Adelman, S.A. *J Chem Phys* 1978, **69**, 3135; 1978, **69**, 3146
8 Burgers, J.M. *Proc Acad Sci (Amsterdam)* 1941, **44**, 1045; 1942, **45**, 9
9 Pyun, C.W. and Fixman, M. *J Chem Phys* 1964, **41**, 937
10 Batcherlor, G.K. *J Fluid Mech* 1972, **52**, 243
11 Vand, V. *J Phys Coll Chem* 1948, **52**, 277
12 Cheng, P.Y. and Schachman, H.K. *J Polym Sci* 1955, **16**, 19
13 Sweeny, K.H. and Geckler, R.D. *J Appl Phys* 1954, **25**, 1135
14 Saunders, F.L. *J Colloid Sci* 1961, **16**, 13
15 McQueen, D. and Hermans, J. *J Coll Interface Sci* 1972, **39**, 389
16 Corti, M. and Degiorgio, V. *Optics Comm* 1975, **14**, 358
17 Cooper, V., Yedgar, S. and Barenholz, Y. *Biochim Biophys Acta* 1974, **363**, 86
18 Mazer, N.A., Benedek, G.B. and Carey, M.C. *J Phys Chem* 1976, **80**, 1075
19 Young, C.Y., Missel, P.J., Mazer, N.A., Benedek, G.B. and Carey, M.C. *J Phys Chem* 1978, **82**, 1375
20 Corti, M. and Degiorgio, V. *Ann Phys* 1978, **3**

21 Koppel, D.E. *J Chem Phys* 1972, **57**, 4814
22 Brown, J.C., Pusey, P.N. and Dietz, R. *J Chem Phys* 1975, **62**, 1136
23 Pusey, P.N. in 'Photon Correlation and Light Beating Spectroscopy', (Ed. H.Z. Cummins, E.R. Pike), Plenum Press, New York, (1974)
24 Altemberger, A.R. and Deutch, J.M. *J Chem Phys* 1973, **59**, 894
25 Tanford, C. 'Physical Chemistry of Macromolecules' John Wiley, New York (1961)
26 Phillies, G.D.J. *J Chem Phys* 1974, **60**, 976
27 Bedeaux, D., Kapral, R. and Mazur, P. *Physica (Utrecht)* 1977, **88A**, 88
28 Candau, S., Young, C.Y., Lemarechal, P. and Bastide, J. *J Chem Phys* (to be published)
29 Cummins, H.Z. in 'Photon Correlation and Light Beating Spectroscopy' (Ed. H.Z. Cummins, E.R. Pike), Plenum Press, New York, (1974)
30 Washburn, E.R., Beguin, A.E. *J Am Chem Soc* 1940, **62**, 579
31 Riess, G., Nervo, J. and Rogez, D. *Polym Prepr* 1977, **18**, 329
32 Griffin, W.C. *J Soc Cosmetic Chem* 1949, **1**, 311